PAPER

Optical Tamm states at the interface between a photonic crystal and an epsilon-near-zero nanocomposite

To cite this article: Stepan Ya Vetrov et al 2017 J. Opt. **19** 085103

View the article online for updates and enhancements.

Related content

- The optical Tamm states at the interface between a photonic crystal and nanoporous silver
R G Bikbaev, S Ya Vetrov and I V Timofeev

- The optical Tamm states at the interface between a photonic crystal and a nanocomposite containing core–shell particles
S Ya Vetrov, P S Pankin and I V Timofeev

- Spectral and polarization properties of a 'cholesteric liquid crystal—phase plate—metal' structure
S Ya Vetrov, M V Pyatnov and I V Timofeev

Recent citations

- Hyperbolic metamaterial for the Tamm plasmon polariton application
Rashid G. Bikbaev et al

- Hybrid Tamm and surface plasmon polaritons in resonant photonic structure
Rashid G. Bikbaev et al

- Transparent conductive oxides for the epsilon-near-zero Tamm plasmon polaritons
Rashid G. Bikbaev et al

Optical Tamm states at the interface between a photonic crystal and an epsilon-near-zero nanocomposite

Stepan Ya Vetrov[1,2], **Rashid G Bikbaev**[1] , **Natalya V Rudakova**[1], **Kuo-Ping Chen**[3] **and Ivan V Timofeev**[2,4]

[1] Institute of Engineering Physics and Radio Electronics, Siberian Federal University, Krasnoyarsk 660041, Russia
[2] Kirensky Institute of Physics, Siberian Branch of the Russian Academy of Sciences, Krasnoyarsk 660036, Russia
[3] Institute of Imaging and Biomedical Photonics, National Chiao Tung University, 301 Gaofa 3rd Road, Tainan 711, Taiwan
[4] Laboratory for Nonlinear Optics and Spectroscopy, Siberian Federal University, Krasnoyarsk 660041, Russia

E-mail: rashid-bikbaev@mail.ru

Abstract
The spectral properties of a one-dimensional photonic crystal bounded with a resonance-absorbing nanocomposite layer are investigated. The bulk concentrations of metal nanoparticles dispersed in a transparent nanocomposite matrix are determined at which the effective permittivity takes near-zero values. The transmission, reflection and absorption spectra of the investigated structures at the normal incidence of light are calculated. The demonstrated possibility of formation of the optical Tamm states at the interface between the photonic crystal and nanocomposite is ensured by the near-zero real and imaginary parts of the permittivity or only the imaginary part of the permittivity at the zero real part. The specific features of field localization at the optical Tamm state frequencies are examined.

Keywords: photonic crystal, nanocomposite, optical Tamm state

(Some figures may appear in colour only in the online journal)

Introduction

In recent years, there has been an increased interest in a special type of surface electromagnetic state in the form of a surface standing wave with zero wavenumber along the interface between media, which does not transfer energy. In this case, the Maxwell equation for the electric field is exactly analogous to the one-electron Schrödinger equation for a semi-infinite crystal, the solution of which is the Tamm surface state. Therefore, the electromagnetic analog of the electronic Tamm state is referred to as the optical Tamm state (OTS) or Tamm plasmon-polariton (TPP). Such states can be observed at the interface between two photonic crystals (PCs) [1, 2] or between a PC and a medium with negative permittivity ε [3, 4]. In experiments, the OTS manifests itself as a narrow peak in the transmission spectrum of a sample [5–7].

The OTSs can be used in sensors and optical switches [8], Faraday- and Kerr-effect amplifiers [9], organic solar cells [10], absorbers [11], thermal emitters [12] and lasers [13]. Gazzano *et al* [14] experimentally showed the possibility of implementation of a single-photon source on the basis of confined Tamm plasmon modes. In [7, 15–17], the OTSs in magnetophotonic crystals were investigated. Gessler *et al* [18] studied the electro-optically tunable Tamm plasmon—exciton—polaritons. The hybrid states were studied in [19]. In our previous work [20], we examined the OTS formation at the interface between a PC bounded by strongly anisotropic
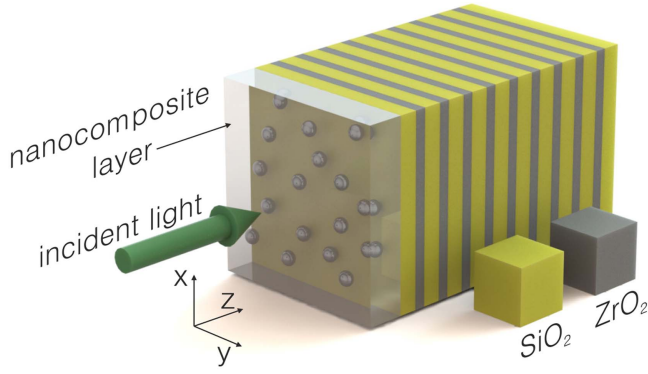
Figure 1. Schematic of a one-dimensional PC conjugated with a nanocomposite layer.

nanocomposite layers from one or two sides. In [21], we proposed a mechanism of the formation of two Tamm states at the interface between a superlattice and a nanoporous silver layer. In [22], the analog of the surface state in a structure containing a cholesteric liquid crystal was found. Later, the chiral OTS was observed in a cholesteric liquid crystal [23]. The metal layer was a polarization-preserving anisotropic metal-dielectric mirror [24].

In conventional TPP, the metal with negative permittivity is needed. However, there has been great interest in the materials with the near-zero permittivity (ENZ) lately. ENZ materials have been used for controlling the wave front shape [25], enhancement of the light transmission through a sub-wavelength aperture [26] and nonlinear effects [27, 28], the fabrication of absorbers [29], photonic wires [30], insulators [31] and third-harmonic generation [32]. Nevertheless, the surface state in PCs and ENZ materials is not well studied yet in the literature. Among the materials with the near-zero permittivity are plasmonic layered structures, ITO, metal-dielectric and polymer nanocomposites, and the composites containing core–shell nanoparticles.

In this study, we demonstrate the possibility of formation of the OTSs at the interface between a PC and a nanocomposite medium. The nanocomposite used consists of metal nanoparticles dispersed in a transparent matrix and has the resonant effective permittivity, while the optical characteristics of the initial materials do not exhibit resonant features [33, 34]. The position of the frequency band corresponding to the near-zero effective permittivity depends on permittivities of the initial materials and bulk nanoparticle concentration, which offers wide opportunities for controlling the optical properties of the OTSs.

Description of the model and determination of transmission

We consider a PC structure in the form of a layered medium bounded by a finite nanocomposite layer (figure 1). A PC unit cell is formed from materials a and b with respective layers thicknesses d_a and d_b and permittivities ε_a and ε_b.

The nanocomposite layer with thickness d_{eff} consists of spherical metal nanoparticles uniformly distributed in the dielectric matrix.

Hereinafter, we assume the PC structure to be placed in vacuum.

The effective permittivity of the nanocomposite is determined from the Maxwell−Garnett formula [35], widely used in studying matrix media [33], in which isolated metal inclusions are dispersed in the matrix material in a small volume fraction

$$\varepsilon_{\text{eff}} = \varepsilon_d\left[1 + \frac{f(\varepsilon_m - \varepsilon_d)}{\varepsilon_d + (1 - f)(\varepsilon_m - \varepsilon_d)1/3}\right], \quad (1)$$

where f is the filling factor, i.e., the fraction of nanoparticles in the matrix; ε_d and $\varepsilon_m(\omega)$ are the permittivities of the matrix and nanoparticle metal, respectively; and ω is the radiation frequency.

The Maxwell−Garnett model suggests the quasi-static approximation. The main features of this model are (i) the electrodynamically isotropic nanocomposite layer and (ii) the size of inclusions and distance between them much smaller than the optical wavelength in the investigated effective medium. The permittivity of the nanoparticle metal can be determined using the Drude approximation

$$\varepsilon_m(\omega) = \varepsilon_0 - \frac{\omega_p^2}{\omega(\omega + i\gamma)}, \quad (2)$$

where ε_0 is the constant that takes into account the contributions of interband transitions of bound electrons, ω_p is the plasma frequency and γ is the reciprocal electron relaxation time.

The light-field variation during passage through each structural layer is determined by the second-order transfer matrix [36] and the transfer matrix of the entire structure, which relates amplitudes of the incident and transmitted waves, is a product of 2×2 matrices

$$M = T_{01}T_{12}...T_{N-1,N}T_{N,S}, \quad (3)$$

where the transfer matrix is

$$T_{n-1,n} = \frac{1}{2}\begin{pmatrix} (1 + h)e^{-i\alpha_n\gamma_n} & (1 - h)e^{i\alpha_n\gamma_n} \\ (1 - h)e^{-i\alpha_n\gamma_n} & (1 + h)e^{i\alpha_n\gamma_n} \end{pmatrix}, \quad (4)$$

Here, $h = (\varepsilon_n/\varepsilon_{n-1})^{1/2}$, $\varepsilon(n)$ is the permittivity of the n layer, $\alpha_n = (\omega/c)\varepsilon(n)^{1/2}$, c is the speed of light, $\gamma_n = z_n - z_{n-1}$ ($n = 1, 2,..., N$) is the layer thicknesses and z_n is the coordinate of the interface between the n layer and the $(n + 1)$ layer adjacent from the right ($\gamma_{N+1} = 0$). The transfer matrix for the orthogonally polarized wave is obtained from equation (4) by changing h for $(\varepsilon_{n-1}/\varepsilon_n)^{1/2}$. The energy transmittance, reflectance and absorbance are determined using the respective formulas

$$T(\omega) = \frac{1}{|\hat{M}_{11}|^2}, \quad R(\omega) = \frac{|\hat{M}_{21}|^2}{|\hat{M}_{11}|^2}.$$
$$A(\omega) = 1 - T(\omega) - R(\omega) \quad (5)$$

where $\hat{M}_{11}$ and $\hat{M}_{21}$ are the elements of matrix $\hat{M}$.
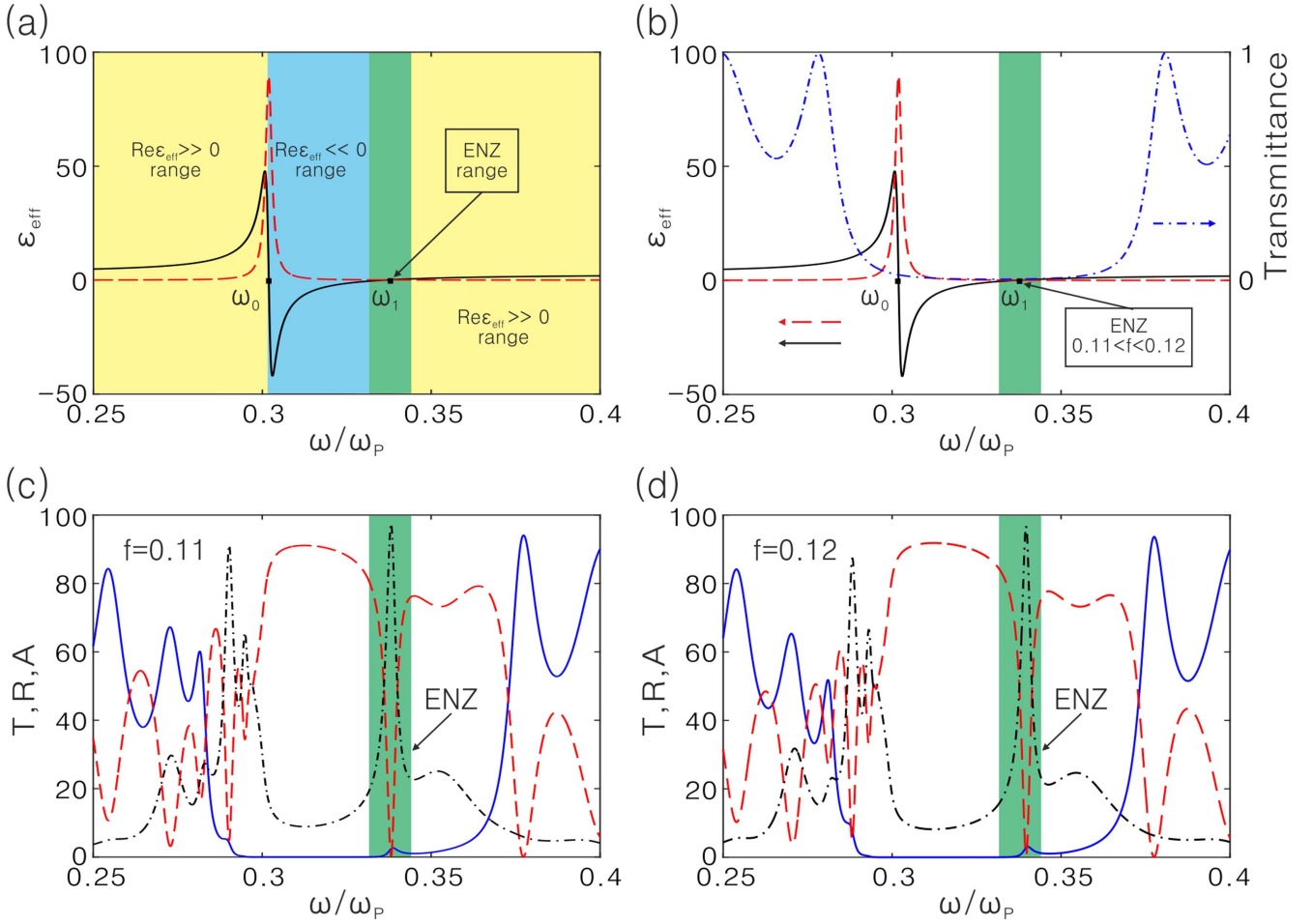
Figure 2. (a) Dependences of the imaginary part *Im* $\varepsilon_{\mathrm{eff}}(\omega)$ (dashed line) and real part *Re* $\varepsilon_{\mathrm{eff}}(\omega)$ (solid line) of the effective permittivity $\varepsilon_{\mathrm{eff}}(\omega)$ on the normalized frequency ω/ω_p. (b) The dashed-and-dotted line shows the transmittance spectrum of the initial PC. The filling factor is $f = 0.11$. Transmittance (solid line), reflectance (dashed line) and absorptance (dashed-and-dotted line) spectra of the PC conjugated with the nanocomposite at $f = 0.11$ (c) and $f = 0.12$ (d). The NC layer thickness is $d_{\mathrm{eff}} = 200$ nm.

Results and discussion

Let us consider the OTSs implemented in the form of standing surface waves at the interface between the nanocomposite—PC. The nanocomposite consists of metal nanospheres dispersed in the dielectric matrix and is characterized by the resonant effective perimittivity $\varepsilon_{\mathrm{eff}}(\omega)$

$$\varepsilon_{\mathrm{eff}}(\omega) = Re\,\varepsilon_{\mathrm{eff}}(\omega) + Im\varepsilon_{\mathrm{eff}}(\omega). \tag{6}$$

Ignoring the small factor γ^2, we find, with the use of (1), the position of frequencies at which the real part of the effective permittivity turns to zero:

$$\omega_0 = \omega_p \sqrt{\frac{1-f}{3\varepsilon_d + (1-f)(\varepsilon_0 - \varepsilon_d)}},$$
$$\omega_1 = \omega_p \sqrt{\frac{1+2f}{(\varepsilon_0 + 2\varepsilon_d + 2f(\varepsilon_0 - \varepsilon_d))}}. \tag{7}$$

At the point $\omega = \omega_0$, the function *Re* $\varepsilon_{\mathrm{eff}}(\omega)$ turns to zero and *Im* $\varepsilon_{\mathrm{eff}}(\omega)$ attains its maximum value; therefore, the localized state at the nanocomposite—PC interface cannot be obtained. We will seek for the OTS in the vicinity of the point $\omega = \omega_1$, since the function *Re* $\varepsilon_{\mathrm{eff}}(\omega)$ at this point also turns to zero and *Im* $\varepsilon_{\mathrm{eff}}(\omega) \ll 1$.

In the range of $[\omega_0, \omega_1]$, we have *Re* $\varepsilon_{\mathrm{eff}}(\omega) \ll 0$; i.e., in this frequency range the nanocomposite is similar to a metal. At frequencies of $\omega < \omega_0$ and $\omega > \omega_1$, we have *Re* $\varepsilon_{\mathrm{eff}}(\omega) \gg 0$ (figure 2(a)).

As materials of the alternating PC levels, we take silicon dioxide SiO$_2$ with a permittivity of $\varepsilon_a = 2.10$ and zirconium dioxide ZrO$_2$ with a permittivity of $\varepsilon_b = 4.16$. The layer thicknesses are $d_a = 74$ nm and $d_b = 50$ nm, respectively, and the number of layers is N = 21.

The dielectric nanocomposite layer with a thickness of $d_{\mathrm{eff}} = 200$ nm consists of silver nanospheres dispersed in transparent optical glass. The parameters of silver are $\varepsilon_0 = 5$, $\omega_p = 9$ eV, and $\gamma = 0.02$ eV and the permittivity of the flint glass (F6) ε_d is constant and equal to 2.56. The frequency
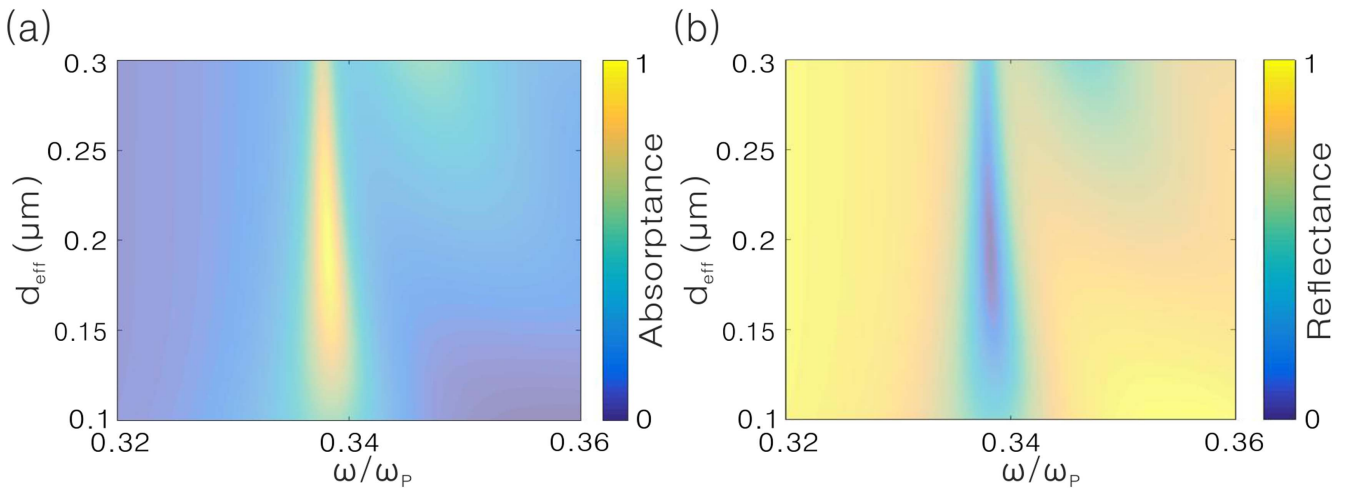
Figure 3. Frequency dependence of the PhC absorption (a) and reflection (b) coefficient at different nanocomposite layer thicknesses. The filling factors of the nanocomposite layer $f = 0.11$.

dependences of the real and imaginary parts of permittivity calculated using formula (1) show that at bulk concentrations of $0.11 < f < 0.12$, the real part of the effective permittivity takes both negative and positive values near the point $\omega = \omega_1$ (figure 2(a)). The use of a nanocomposite film with a bulk nanosphere concentration beyond this range leads to the shift of the OTS frequency toward larger $Re\ \varepsilon_{\mathrm{eff}}$ absolute values (see [3, 20] for more details). As an example, figure 2(a) shows the dependences $Im\ \varepsilon_{\mathrm{eff}}(\omega)$ and $Re\ \varepsilon_{\mathrm{eff}}(\omega)$ for $f = 0.11$. In addition, figure 2(b) presents the seed PC spectrum, including the band gap region.

It can be seen that the frequency band where the real part of the effective permittivity takes the near-zero values lies in the band gap of the initial PC. The wavelength corresponding to the frequency ω_1 is $\lambda = 405.8$ nm.

The transmittance, reflectance and absorptance spectra at the normal incidence of light on the PC conjugated with the nanocomposite layer for the cases of $f = 0.11$ and $f = 0.12$ are presented in figures 2(c) and (d). It can be seen that near the high-frequency boundary of the PC band gap, the absorption band arises, which corresponds to the Tamm state localized at the nanocomposite—PC interface. It corresponds to the leaky state phase matching condition, stating that the product of reflection amplitudes is real:

$$r_{PC} r_{NC} \in R. \qquad (8)$$

A resonant mechanism of almost perfect absorption [11, 37] can be explained introducing a critical coupling of OTS to the relaxation channels [38, 39]. A small value of the speed of energy leakage through the channel of the photonic crystal (transmission 3%) leads to the equality of energy leakages in channels of the pumping and the nanocomposite absorption. Under this critical coupling condition, the incident radiation is completely absorbed by the nanocomposite. To tune the critical coupling, one can change the number of photonic crystal periods or the nanocomposite layer thickness (figure 3).

Analysis of figure 3 shows that the nanocomposite layer thickness variation leads to critical coupling violation and reduces the absorption at the OTS frequency.

The established OTSs exist in an extremely narrow frequency band, where the real part of the effective permittivity is close to zero. In particular, the effective permittivities at the OTS frequencies for filling factors of $f = 0.11$ and $f = 0.12$ are $\varepsilon_{\mathrm{eff}}(\omega) = 0.023 + 0.085i$ and $\varepsilon_{\mathrm{eff}}(\omega) = -0.007 + 0.081i$, respectively. A comparison of the reflectance spectra and electric field intensity distribution at the corresponding OTS frequencies for the PC contacting with the nanocomposite film is illustrated in figure 4.

It can be seen that the field localization at the OTS frequencies in the cases $Re\ \varepsilon_{\mathrm{eff}}(\omega) > 0$ and $Re\ \varepsilon_{\mathrm{eff}}(\omega) < 0$ is nearly the same. In both cases, the OTS light field is concentrated in the area comparable with the wavelength. The wavelengths corresponding to the reflectance minima differ by 1.8 nm.

It should be noted that the OTS is formed not only at the negative real part of the effective permittivity of the nanocomposite, but also at the positive ones.

The decrease in the field of the mode localized at the interface deep into the nanocomposite is caused by the negative dielectric permittivity $Re\ \varepsilon_{\mathrm{eff}}(\omega) \ll 0$ of the nanocomposite, at which the latter is similar to a metal, and the decrease in the field deep into the PC results from the damping of the Bloch wave at the band gap frequency, or, in other words, is related to the Bragg reflection at the interface with the periodic layered medium. We propose the following explanation of the OTS formation at the positive nanocomposite permittivity. Figure 5 shows the calculated dependence of the Fresnel reflection on $Re\ \varepsilon_{\mathrm{eff}}$ for the normal incidence of light on a semi-infinite media, i.e., silicon dioxide adjacent to the nanocomposite. It can be seen that at small positive and small negative $Re\ \varepsilon_{\mathrm{eff}}(\omega)$ values, the Fresnel reflection from the nanocomposite attains 50%, which facilitates the formation of a localized state at the PC-nanocomposite interface in both cases. In view of the
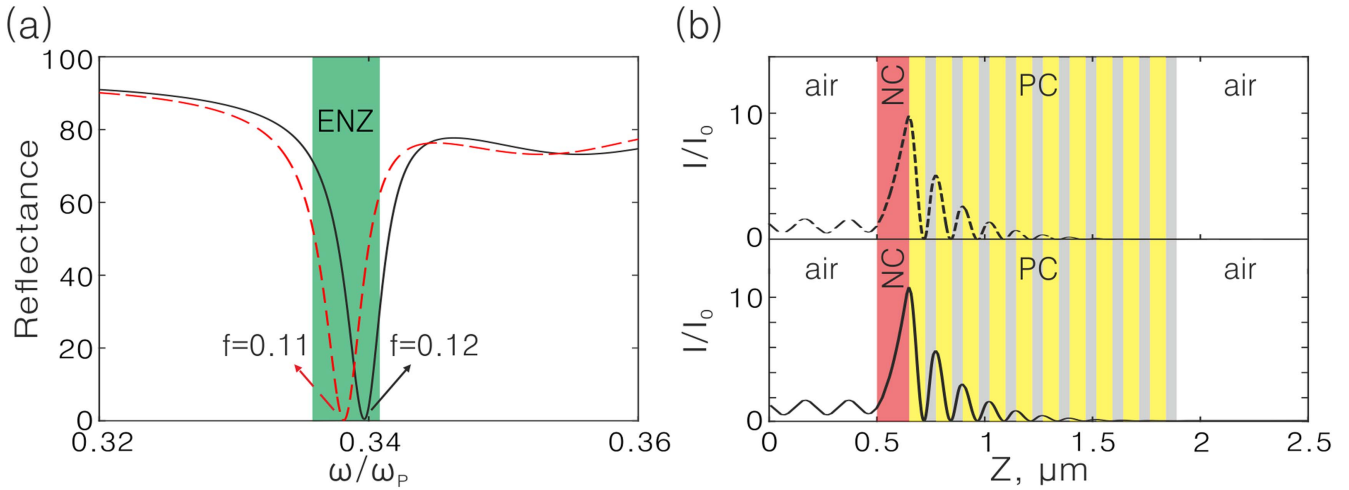
Figure 4. (a) Reflectance spectra of the nanocomposite—PC structure at the normal incidence of light on the sample. (b) Schematic of a one-dimensional PC conjugated with the nanocomposite layer and field intensity distribution at the OTS frequency normalized to the input intensity. The nanocomposite layer thickness is $d_{\text{eff}} = 200$ nm and the filling factors are $f = 0.11$ (dashed line) and $f = 0.12$ (solid line).
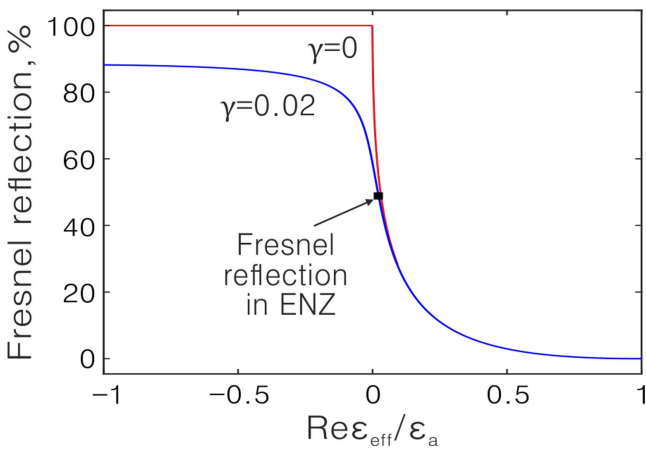
Figure 5. Fresnel reflection at the nanocomposite-silicon dioxide interface. The nanocomposite filling factor is $f = 0.11$.

aforementioned, one can expect that at the near-zero values of $Re\ \varepsilon_{\text{eff}}(\omega) > 0$ and $Re\ \varepsilon_{\text{eff}}(\omega) < 0$, the field localization at the OTS frequencies will be nearly the same. This conclusion was confirmed by the calculation (figure 4(b)).

According to (7), the position of frequency ω_1 is sensitive to the variation in the nanocomposite filling factor. Figure 6(a) presents reflectance spectra of the PC structure at a specified nanocomposite thickness and different filling factors f. It can be seen that as the volume fraction of nanospheres increases from 11% to 12%, the OTS frequency shifts to the high-frequency region. In this case, we have $Re\ \varepsilon_{\text{eff}}(\omega) > 0$ up to the filling factor value of $f = 0.116$ ($\omega = 0.3396\omega_p$), at which $\varepsilon_{\text{eff}}(\omega) = 0.006 + 0.082i$. The transition to the region $Re\ \varepsilon_{\text{eff}}(\omega) < 0$ occurs at $f > 0.118$. At the bulk concentration of $f = 0.118$ ($\omega = 0.3399\omega_p$), we have $Re\ \varepsilon_{\text{eff}}(\omega) = 0$ and the effective permittivity at this frequency is $\varepsilon_{\text{eff}}(\omega) = 0 + 0.082i$ (figure 6(b)).

Study of the field localization at the OTS frequency at zero real part of the effective permittivity showed that the field intensity normalized to the input intensity takes the same values as in figure 4(b). Note the weak dependence of $Im\ \varepsilon_{\text{eff}}(\omega)$ on the bulk concentration of nanospheres in the investigated frequency range (figure 6(b)). This results in almost constant absorption of the nanocomposite—PC structure at about 97%.

An effective way to control energy spectra of PC structures is tuning the angle of light incidence. The reflection spectra at oblique light incidence are shown in figure 7.

The PC band gap shifts to the shorter wavelength region for TE wave when the electric field is transverse to the light incidence plane. In this case, the OTS also shifts to shorter wavelength. For TM wave the picture is more complicated. The shift of bang gap into the short wavelength region is more sharp. The band gap and the negative permittivity region of the nanocomposite cease to overlap at angles larger than 35 degrees. As a result, the OTS disappears.

Conclusions

The spectral properties of the one-dimensional PC bounded on one side by the resonant-absorbing nanocomposite layer consisting of spherical silver nanoparticles dispersed in transparent optical glass were studied by the transfer matrix technique.

The possibility of formation of the OTSs at the PC-nanocomposite interface with the near-zero permittivity was numerically demonstrated. It was shown that these states can form at finite negative and positive real parts of the permittivity, as well as in the case when the real part of the permittivity turns to zero. The absorption of the nanocomposite in the frequency region with the near-zero permittivity weakly depends on the filling factor and amounts
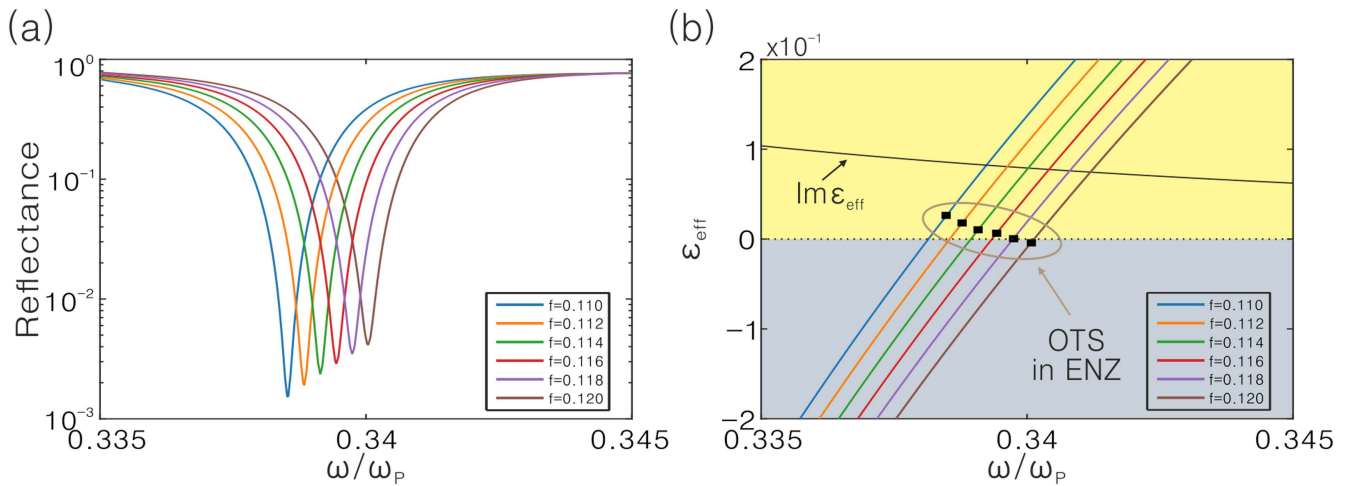
Figure 6. (a) Reflectance spectra of the nanocomposite—PC structure. (b) Dependences of the imaginary part *Im* $\varepsilon_{eff}(\omega)$ and real part *Re* $\varepsilon_{eff}(\omega)$ of the effective permittivity $\varepsilon_{eff}(\omega)$ on the normalized frequency ω/ω_p at different filling factors *f*. Dots in figure 6(b) show the real part of the effective permittivity at the OTS frequencies. The nanocomposite layer thickness is $d_{eff} = 200$ nm.
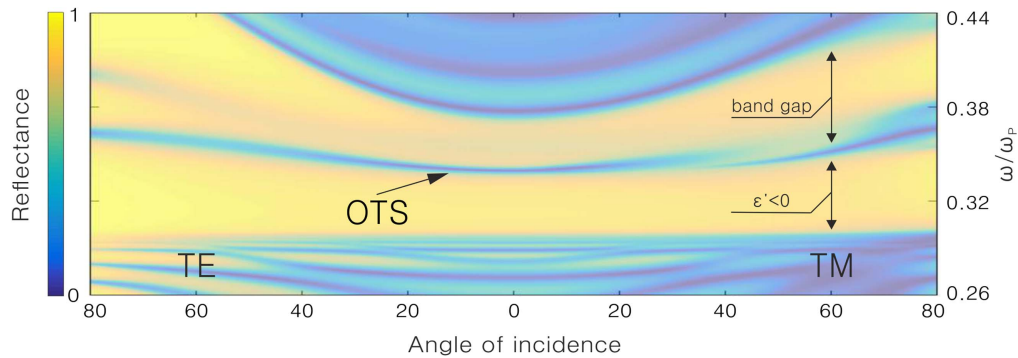
Figure 7. Angular and frequency dependence of the PhC reflection coefficient for the TE and TM waves. The nanocomposite layer thickness $d_{eff} = 200$ nm and the filling factors $f = 0.118$.

to about 97%. It was established that in all the investigated cases the field distribution in the OTS at the PC-nanocomposite interface is almost the same. The results obtain develop the idea about OTS implementation in the nanocomposite—PC structures.

ORCID

Rashid G Bikbaev ⓘ https://orcid.org/0000-0002-0549-5917

References

[1] Vinogradov A P, Dorofeenko A V, Merzlikin A M and Lisyansky A A 2010 *Phys. Usp.* **53** 243
[2] Kavokin A V, Shelykh I A and Malpuech G 2005 *Phys. Rev. B* **72** 233102
[3] Vetrov S Y, Bikbaev R G and Timofeev I V 2013 *JETP* **117** 988
[4] Kaliteevski M, Iorsh I, Brand S, Abram R A, Chamberlain J M, Kavokin A V and Shelykh I A 2007 *Phys. Rev. B* **76** 165415
[5] Sasin M E, Seisyan R P, Kalitteevski M A, Brand S, Abram R A, Chamberlain J M, Egorov A Y, Vasil'ev A P, Mikhrin V S and Kavokin A V 2008 *Appl. Phys. Lett.* **92** 251112
[6] Sasin M E, Seisyan R P, Kalitteevski M A, Brand S, Abram R A, Chamberlain J M, Egorov A Y, Vasil'ev A P, Mikhrin V S and Kavokin A V 2010 *Superlattices Microstruct.* **47** 44
[7] Goto T, Dorofeenko A V, Merzlikin A M, Baryshev A V, Vinogradov A P, Inoue M, Lisyansky A A and Granovsky A B 2008 *Phys. Rev. Lett.* **101** 113902
[8] Zhang W L and Yu S F 2010 *Opt. Comm.* **283** 2622
[9] Vinogradov A P, Dorofeenko A V, Erokhin S G, Inoue M, Lisyansky A A, Merzlikin A M and Granovsky A B 2006 *Phys. Rev. B* **74** 045128

[10] Zhang X-L, Song J-F, Li X-B, Feng J and Sun H-B 2012 *Appl. Phys. Lett.* **101** 243901

[11] Gong Y, Liu X, Lu H, Wang L and Wang G 2011 *Opt. Express* **19** 18393

[12] Yang Z Y, Ishii S, Yokoyama T, Dao T D, Sun M G, Nagao T and Chen K P 2016 *Opt. Lett.* **41** 4453

[13] Symonds C, Lheureux G, Hugonin J P, Greffet J J, Laverdant J, Brucoli G, Lemaitre A, Senellart P and Bellessa J 2013 *Nano Lett.* **13** 3179

[14] Symonds C, Lemaître A, Senellart P, Jomaa M H, Aberra Guebrou S, Homeyer E, Brucoli G and Bellessa J 2012 *Appl. Phys. Lett.* **100** 121122

[15] Dong H Y, Wang J and Cui T J 2013 *Phys. Rev.* B **87** 045406

[16] Da H, Bao Q, Sanaei R, Teng J, Loh K P, Garcia-Vidal F J and Qiu W 2013 *Phys. Rev.* B **88** 205405

[17] Khokhlov N E *et al* 2015 *J. Phys. D: Appl. Phys.* **48** 095001

[18] Gessler J, Baumann V, Emmerling M, Amthor M, Winkler K, Höfling S, Schneider C and Kamp M 2014 *Appl. Phys. Lett.* **105** 181107

[19] Fang Y-T, Ni Y-X, He H-Q and Hu J-X 2014 *Opt. Comm.* **320** 99–104

[20] Vetrov S Y, Bikbaev R G and Timofeev I V 2016 *Opt. Comm.* **395** 275–81

[21] Bikbaev R G, Vetrov S Y and Timofeev I V 2017 *J. Opt.* **19** 015104

[22] Vetrov S Y, Pyatnov M V and Timofeev I V 2014 *Opt. Lett.* **39** 2743

[23] Timofeev I V and Vetrov S Y 2016 *JETP Lett.* **104** 380

[24] Rudakova N V, Timofeev I V and Vetrov S Y 2017 *Bull. Russ. Acad. Sci.: Phys.* **81** 5

[25] Alu A, Silveirinha M G, Salandrino A and Engheta N 2007 *Phys. Rev.* B **75** 155410

[26] Inampudi S, Adams D C, Ribaudo T, Slocum D, Vangala S, Goodhue W D, Wasserman D and Podolskiy V A 2014 *Phys. Rev.* B **89** 125119

[27] Ciattoni A, Rizza C, Marini A, Di Falco A, Faccio D and Scalora M 2016 *Laser Photon. Rev.* **10** 517

[28] Kaipurath R M, Pietrzyk M, Caspani L, Roger T, Clerici M, Rizza C, Ciattoni A, Di Falco A and Faccio D 2016 *Sci. Rep.* **6** 27700

[29] Park J, Kang J-H, Liu X and Brongersma M L 2015 *Sci. Rep.* **5** 15754

[30] Liu R, Roberts C, Zhong Y, Podolskiy V A and Wasserman D 2016 *ACS Photon.* **3** 1045–52

[31] Davoyan A R, Mahmoud A M and Engheta N 2013 *Opt. Express* **21** 3279

[32] Luk T S, Ceglia D, Liu S, Keeler G A, Prasankumar R P, Vincenti M A, Scalora M, Sinclair M B and Campione S 2015 *Appl. Phys. Lett.* **106** 151103

[33] Oraevskii A N and Protsenko I E 2001 *Quantum Elect.* **31** 252

[34] Sihvola A H 2008 *Electromagnetic Mixing Formulas and Applications* (London: Institution of Engineering and Technology)

[35] Maxwell Garnett J C 1904 *Phil. Trans. R. Soc.* A **203** 385–420

[36] Yeh P 1979 *J. Opt. Soc. Am.* **69** 742

[37] Landy N I, Sajuyigbe S, Mock J J, Smith D R and Padilla W J 2008 *Phys. Rev. Lett.* **100** 207402

[38] Auguié B, Bruchhausen A and Fainstein A 2015 *J. Opt.* **17** 35003

[39] Haus H A 1983 *Waves and Fields in Optoelectronics* (Upper Saddle River, NJ: Prentice Hall)